Loss of Cxcl12/Sdf-1 in adult mice decreases the quiescent state of hematopoietic stem/progenitor cells and alters the pattern of hematopoietic regeneration after myelosuppression

Yi-Shiuan Tzeng,[1,2] Hung Li,[1,2] Yuan-Lin Kang,[3] Wen-Cheng Chen,[1,2] Wei-Cheng Cheng,[2] and Dar-Ming Lai[4]

[1]Institute of Biochemistry and Molecular Biology, National Yang-Ming University, Taipei, Taiwan; [2]Institute of Molecular Biology, Academia Sinica, Taipei, Taiwan; [3]Department of Genetics, Cell Biology and Development, University of Minnesota, Minneapolis, MN; and [4]Division of Neurosurgery, Department of Surgery, National Taiwan University Hospital, Taipei, Taiwan

The C-X-C-type chemokine Cxcl12, also known as stromal cell–derived factor-1, plays a critical role in hematopoiesis during fetal development. However, the functional requirement of Cxcl12 in the adult hematopoietic stem/progenitor cell (HSPC) regulation was still unclear. In this report, we developed a murine Cxcl12 conditional deletion model in which the target gene can be deleted at the adult stage. We found that loss of stroma-secreted Cxcl12 in the adult led to expansion of the HSPC population as well as a reduction in long-term quiescent stem cells. In Cxcl12-deficient bone marrow, HSPCs were absent along the endosteal surface, and blood cell regeneration occurred predominantly in the perisinusoidal space after 5-fluorouracil myelosuppression challenge. Our results indicate that Cxcl12 is required for HSPC homeostasis regulation and is an important factor for osteoblastic niche organization in adult stage bone marrow. (*Blood*. 2011; 117(2):429-439)

Introduction

The hematopoietic system, one of the largest organ systems in mammals, is comprising several types of blood cells, each with a finite life span. The replenishment of blood cells depends on the quiescent hematopoietic stem cells (HSCs), which constitute a small subset of hematopoietic stem/progenitor cell (HSPC) pool located in bone marrow (BM). In adult BM, HSPCs are located in a specialized microenvironment, also called the "stem cell niche," where HSPC pool is kept in a homeostatic state.[1] In the niche microenvironment, extracellular signals exert critical effects on HSPC homeostasis.[2,3] Among others, the *C-X-C* type chemokine ligand 12 (Cxcl12), also known as stromal cell–derived factor-1, has drawn much attention due to its unique biologic function to regulate stem cell migration and survival.[4] In adult BM, Cxcl12 is expressed in a variety of mesenchymal cells, including osteoblasts,[5,6] endothelium,[7] and certain types of reticular cells.[8] In cell cultures, Cxcl12 is expressed in primary BM stromal cells and other stromal cell lines.[9,10] The findings raise the possibility that Cxcl12 plays as a significant niche factor and is involved in the maintenance of the HSPC pool. Genetic studies revealed that targeted deletion of Cxcl12 or of one of its receptors, Cxcr4, results in a failure to initiate BM hematopoiesis,[11,12] highlighting their importance in the BM hematopoiesis ontogeny. In adult mice, loss of Cxcr4 disrupted the HSPC homeostasis.[8,13] However, there was still lack of information regarding the ligand deficiency in the hematopoietic system and the possible phenotypic change of the BM niche microenvironment.

To investigate the role of Cxcl12 directly in the adult stage, we used a conditional gene targeting strategy to bypass the perinatal lethality of *Cxcl12* homozygote mutant phenotype and ablate the target gene in the adult. We hypothesized that the loss of Cxcl12 would affect the HSPC homeostasis and niche organization. Our results showed that stromal cell–secreted Cxcl12 participated in HSPC homeostasis. In the physiologic state, loss of Cxcl12 led to increased size of the progenitor cell pool in BM in conjunction with a reduction of long-term HSCs. We also found that the loss of Cxcl12 affected the HSPC lodgment to bone-lining surface. Upon myelosuppression, the BM hematologic regeneration occurred mostly in the perisinusoidal space instead of on the endosteal surface in Cxcl12-deficient mice.

Methods

Mice

The embryonic stem cell electroporation and blastocyst injection were performed by the Transgenic Core Facility at the Institute of Molecular Biology, Academia Sinica. Primers for genotyping are listed in supplemental Table 1 (available on the *Blood* Web site; see the Supplemental Materials link at the top of the online article). The E2A-Cre transgenic, CAG-enhanced green fluorescent protein (EGFP) transgenic, TgCAGGCreER, and CD45.1 syngeneic mice were purchased from The Jackson Laboratory and were maintained in a 129svJ/C57BL/6J background. Mice were bred in a specific pathogen–free environment following the guidelines issued by the Academia Sinica Institutional Animal Care and Utilization Committee.

PB sample collection

For the peripheral blood (PB) cell profile, 200 μL of blood were collected by retro-orbital puncture using heparin-coated capillaries and analyzed by an Abbott Cell-Dyn 3700 hematology analyzer.

Bone marrow transplantation

The genotypes of donor and recipient mice are described in the Results. Recipient mice first received 1000 cGy total body irradiation. Within

Submitted January 26, 2010; accepted August 26, 2010. Prepublished online as *Blood* First Edition paper, September 10, 2010; DOI 10.1182/blood-2010-01-266833.

An Inside *Blood* analysis of this article appears at the front of this issue.

The online version of this article contains a data supplement.

The publication costs of this article were defrayed in part by page charge payment. Therefore, and solely to indicate this fact, this article is hereby marked "advertisement" in accordance with 18 USC section 1734.

24 hours, 100 μL of minimal essential medium-α (Invitrogen) containing 5×10^6 donor cells were administered by retro-orbital injection. For some experiments, mice received 6 doses of tamoxifen at 1-day intervals 8 weeks after transplantation.

Side population assay, Hoechst 33342/Pyronin Y dual stain and flow cytometry

The fluorochrome-conjugated antibodies used in each assay are listed in supplemental Table 2. For side population (SP) analysis, we followed the method described by Goodell et al[14]; Lineage$^-$Sca1$^+$c-Kit$^+$ (LSK) antibody staining was performed after the Hoechst 33342 reaction. Cell-cycle analysis using Hoechst 33342/Pyronin Y was described by Ladd et al.[15] Briefly, BM cells were treated with 1 μg/mL of Hoechst 33342 for 45 minutes followed by 1 μg/mL of Pyronin Y for another 45 minutes. Cells were further stained with LSK antibodies. The flow cytometry of stained cells were performed on the LSRII flow cytometer (BD Bioscience), and data were analyzed by FlowJo Version 7.2.2 software (TreeStar).

BrdU incorporation assay

One dose of 3 mg of BrdU (5-bromo-2-deoxyuridine; Sigma-Aldrich) was intraperitoneally injected into mice, and BM samples were collected 3 days thereafter. For 14-day labeling, BrdU was administered in the drinking water at 1 mg/mL until day of sacrifice.

Colony-forming assay

BM or PB cells were cultured in duplicate in semisolid methylcellulose-based medium (MethoCult M3434, StemCell Technologies) as instructed by the manufacturer. Total colonies were counted 9 days after seeding under an inverted microscope (Olympus).

Preparation of BM stromal cells and LTC-IC assay

The genotypes of stromal cells and tested BM samples are described in the Results. Briefly, BM stromal cells were cultured in long-term culture medium M5300 with 10^{-6} M hydrocortisone (both from StemCell Technologies). Thirteen days after seeding, cells were treated with 0.5 μM 4-hydroxytamoxifen (4-OHT) (Sigma-Aldrich). Two days after 4-OHT treatment, cells were then inactivated by 1500 cGy γ-irradiation. BM cells were harvested from test mice and seeded onto the stromal layer in a 2-fold serial dilution from 10^5 to 3.125×10^3 per well, each dilution with 10 replicates. Forty days after test cell seeding, 100 μL MethoCult M3434 medium was added into each well. Colonies were observed 9 days later. The limiting-dilution analysis software L-Calc Version 1.1 (StemCell Technologies) was used to analyze the frequency of LTC-ICs in each cell population.

Histology and immunofluorescence

Fresh femurs were collected, and frozen sections were prepared by the tape transfer method (Section-Lab Co Ltd). For hematoxylin and eosin staining, sections were pretreated with 4% paraformaldehyde. For immunofluorescence studies, sections were treated with 100% ethanol and blocked in 2% horse serum. Primary antibodies are as follows: goat anti–Cxcl12/ stromal cell–derived factor-1 (Santa Cruz Biotechnology), rabbit anti-osteocalcin (Takara), rat anti-Tie2 (Biolegend), fluorescein isothiocyanate (FITC)–conjugated mouse anti-CD45.2 (Biolegend), FITC-conjugated rat anti-cKit (BD Bioscience), phycoerythrin-conjugated rat anti–Sca-1 (BD Bioscience), and biotinylated rat anti–MECA-32 (mouse panendothelial cell antigen, clone 32; BD Bioscience). For secondary antibodies, we used Alexa Fluor 488 anti–rabbit immunoglobulin G and Alexa Fluor 546 anti–goat or anti–rat immunoglobulin G. Biotinylated antibody was visualized by strepavidin-Cy5 conjugate (all from Invitrogen). For immunostaining of CD150/CD41/CD48/osteocalcin, sections were air-dried overnight and fixed by ice-cold acetone for 10 minutes. Sections were blocked by 5% fetal bovine serum and stained for rat anti-CD150 antibody (TC15-12F12.2, BioLegend) and anti-osteocalcin or anti–MECA-32 antibody as described above. After washing, Alexa Fluor 546–conjugated anti-rat (Invitrogen) and Alexa Fluor 647–conjugated anti-rabbit antibodies were used to visualize CD150 and osteocalcin, respectively. Sections were further blocked again by 1% rat serum and then stained for FITC-conjugated CD41 (MWReg30, eBioscience) and CD48 (HM48-1, eBioscience) antibodies. All immunofluorescence sections were counterstained by DAPI (4,6 diamidino-2-phenylindole). Photos were taken on Zeiss Axioimager Z-1 and Zeiss LSM 510, and images were processed in Zeiss ZEN Version 6.0.0.233 software.

Quantitative RT-PCR

Primers for target genes are listed in supplemental Table 3. Target genes were amplified by SYBR Premix Ex Taq (Takara), and polymerase chain reaction (PCR) was performed on a LightCycler 1.2 quantitative PCR machine (Roche). Gene expression level was normalized to the level of glyceraldehyde 3-phosphate dehydrogenase (GAPDH) or β-actin expression of each sample.

ELISA

Protein concentration in stromal culture medium was determined by enzyme-linked immunosorbent assay (ELISA). The ELISA kit for Cxcl12 and stem cell factor (SCF) were purchased from R&D Systems, and their instructions were followed.

Statistical analysis

In vitro and in vivo experiments were independently performed at least 3 times with similar results. Data were processed in GraphPad Prism 4 software (GraphPad Software) and expressed as mean ± SEM in each bar graph. Student *t* test was used to evaluate the significance value.

Results

Generation of *Cxcl12* conditional allele

We made a genetically engineered allele of *Cxcl12* in which the coding exon was flanked by 2 LoxP sequences (supplemental Figure 1A). The alleles described in this report are illustrated in supplemental Figure 1B. The removal of the neomycin cassette and the generation of a *Cxcl12* floxed allele and a minus allele were achieved by mating to the E2A-Cre transgenic mice. To introduce Cre activity, we used the TgCAGGCreER transgenic mice expressing a ubiquitously expressed, tamoxifen-inducible CreER fusion protein.[16] We scheduled a mating strategy to generate Cxcl12$^{F/+}$;TgCAGGCreER (abbreviated as Cxcl12$^{F/+}$;Tg in the following sections) and Cxcl12$^{F/-}$;TgCAGGCreER (Cxcl12$^{F/-}$;Tg) offspring. We then induced the *Cxcl12* floxed allele deletion by administering tamoxifen at the neonatal stage. A single tamoxifen injection (150 μg/g body weight) was given to postnatal day 7 neonates, and samples were collected 7 days after treatment. *Cxcl12* was ablated successfully at the genomic level as assayed by genomic Southern blot (supplemental Figure 1C). Quantitative RT-PCR revealed a more than 95% reduction of Cxcl12 transcript level in major organs (supplemental Figure 1D left panel). For description, we designated tamoxifen- or 4-OHT–treated Cxcl12$^{F/+}$;Tg and Cxcl12$^{F/-}$;Tg mice or samples as "Cxcl12 WT" and "Cxcl12-cKO," respectively.

To test the applicability of this system in the adult stage, we administered 6 doses of tamoxifen (150 μg/g body weight) to 10-week-old mice in 1-day intervals. Quantitative RT-PCR of BM samples revealed that the Cxcl12 transcript remained comparable in Cxcl12 wild-type (Cxcl12-WT) mice 2 weeks after tamoxifen treatment. At the same time, Cxcl12 transcript in Cxcl12 knockout (Cxcl12-cKO) mice dropped to less than 5% of that in Cxcl12-WT

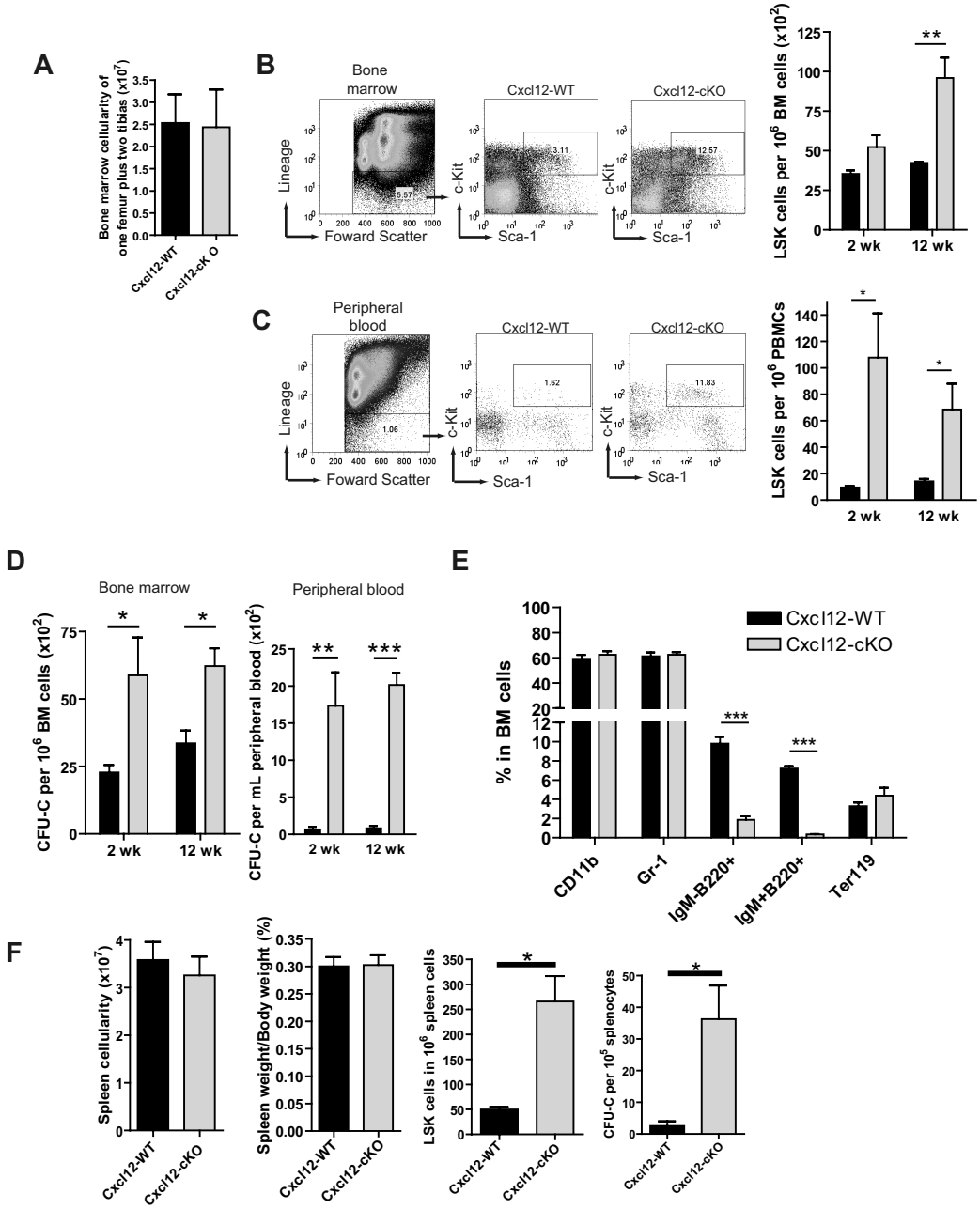

Figure 1. Cxcl12 deficiency leads to hematopoietic progenitor pool expansion in BM. (A) 12 weeks (wks) after tamoxifen treatment, there was no significant change of the total number of BM nucleated cells between Cxcl12-WT (n = 10) and Cxcl12-cKO mice (n = 11) (mean ± SEM; $P = .812$). (B-C) Representative figures of the gating of $Lin^-Sca\text{-}1^+c\text{-}Kit^+$ (LSK) cell populations in BM (B) or peripheral blood mononuclear cells (PBMCs) (C) of Cxcl12-WT and Cxcl12-cKO mice 2 wks or 12 wks after tamoxifen treatment. Right panel shows the percentage of LSK cells in BM or PB (mean ± SEM; $*P < .05$, $**P < .005$; n = 6 each). (D) Statistical bar graphs of colony forming unit cell (CFU-C) assay of BM and PB derived from Cxcl12-WT and Cxcl12-cKO mice 2 and 12 wks after tamoxifen treatment (means ± SEM; $*P < .05$, $**P < .005$, $***P < .001$; n = 6 each group). (E) Lineage-specific marker analysis for BM cells from Cxcl12-WT and Cxcl12-cKO mice 12 wks after tamoxifen treatment. Data are expressed as mean ± SEM ($***P < .001$; n = 3). (F) Spleen cellularity, spleen/body weight ratio, spleen LSK cells, and CFU-C counts in spleen were examined 12 wks after tamoxifen treatment (mean ± SEM; $*P < .05$; for spleen cellularity and spleen/body weight ratio n = 10 each, for LSK and CFU-C n = 4 each). For all bar graphs, black bars are Cxcl12-WT and gray bars are Cxcl12-cKO.

mice (supplemental Figure 1E). We also tested the Cxcl12 transcript in other major organs (supplemental Figure 1D right panel) and found that in adult mice, Cxcl12 was significantly expressed in the kidney, liver, and heart. Tamoxifen-activated DNA recombination was more efficient in hematopoietic organs in which Cxcl12 transcripts in the BM and spleen were reduced to less than 5% of those in the WT counterpart. Immunofluorescence study also revealed that in Cxcl12-WT BM, Cxcl12 were expressed at the osteocalcin-positive osteoblasts; in Cxcl12-cKO BM, Cxcl12 signal was not detected at these osteoblasts or other cells with identifiable cell morphology (supplemental Figure 2).

Loss of Cxcl12 leads to expansion of hematopoietic progenitor pool

Cxcl12 is a critical factor mediating HSPC migration during the mice embryonic stage.[17] We hypothesized that loss of Cxcl12 could also affect the adult stage hematopoiesis. To address this question,

Table 1. Peripheral blood cell profile of Cxcl12-WT and Cxcl12-cKO mice

Lineage	Cxcl12-WT (n = 6)	Cxcl12-cKO (n = 7)
WBC, $\times 10^3/\mu L$	7.82 ± 0.5906	7.057 ± 0.8148
Neutrophil (%)	16.1 ± 0.7572	22.01 ± 2.105*
Monocyte (%)	5.184 ± 1.222	3.577 ± 1.318
Lymphocyte (%)	75.38 ± 2.035	69.5 ± 4.136
RBC, $\times 10^6/\mu L$	8.937 ± 0.3209	9.392 ± 0.2936
Platelet, $\times 10^3/\mu L$	838.2 ± 80.2	893.5 ± 65.45

WBC indicates white blood cell; and RBC, red blood cell.
*$P < .05$.

we first measured the blood profiles in BM and PB in Cxcl12-cKO and Cxcl12-WT mice. Twelve weeks after tamoxifen treatment, we found that the BM cellularity did not change significantly (Figure 1A). In PB, the blood cell profile was also minimally changed despite a modest but significant increase in the percentage of circulating neutrophils in Cxcl12-cKO mice (Table 1). To measure the potential changes of the precursor compartment, we set up flow cytometric analysis using the criteria of LSK surface markers to identify the progenitor cell pool. We found a moderate increase of LSK cells in the Cxcl12-cKO BM (Figure 1B) and a dramatic increase in PB (Figure 1C) after tamoxifen treatment. These findings were further confirmed by in vitro colony forming unit cell counts (Figure 1D). A similar phenotype was observed in the spleen where LSK cells and colony forming unit cells were both elevated by 5-fold and 15-fold, respectively, while the total spleen cellularity or the spleen-versus-body weight ratio between Cxcl12-WT and -cKO mice remained comparable (Figure 1F). In lineage analysis, B-cell progenitors, identified as IgM^-B220^+ and IgM^+B220^+ cells, were significantly reduced in BM from the Cxcl12-cKO mice while the percentage of $CD11b^+$, $Gr\text{-}1^+$ myeloid cells and $Ter119^+$ erythroblasts were similar in both genotypes (Figure 1E). These results revealed that loss of Cxcl12 led to an increased hematopoietic progenitor population in BM, PB, and the spleen. In addition, B-cell development in adult stage BM was critically dependent on Cxcl12, while other cell lineage precursors were seemingly less affected by loss of Cxcl12 under physiologic state.

Loss of Cxcl12 leads to hematopoietic progenitor pool expansion at the expense of long-term HSCs

To identify the HSCs in the total HSPC pool, we used Hoechst 33342 SP analysis.[14] Before and 2 weeks after tamoxifen treatment, the percentage of SP cells in BM was comparable between the 2 genotypes; however, the SP cell numbers gradually decreased in Cxcl12-cKO mice, and there was nearly a 3.5-fold reduction of SP cells 12 weeks after tamoxifen treatment (Figure 2A). Supporting this finding, the LSK population from Cxcl12-cKO mice also contained a smaller percentage of the cells with SP characteristics (Figure 2B). Using CD34/Flt3/LSK analysis,[18] we also found that there was a 1.5-fold fewer percentage of $CD34^-Flt3^-LSK$ long-term HSCs and a concomitant higher percentage of $CD34^+Flt3^-LSK$ short-term HSCs in Cxcl12-cKO samples (Figure 2C).

In addition to flow cytometric analysis, we set up a LTC-IC assay and in vivo competitive repopulation assay.[19] Twelve weeks after tamoxifen treatment, we seeded the BM cells from Cxcl12-WT or Cxcl12-cKO mice onto the wild-type BM stromal layer. Consistent with the flow cytometric results, the LTC-IC readout was also significantly reduced in the Cxcl12-cKO BM samples (Figure 2D). The competitive repopulation assay demonstrated that the $CD45.2^+$ Cxcl12-WT cells competed with the equal number of $CD45.1^+$ wild-type competitors and constituted approximately 50% of the BM LSK population or the total BM cells, while the $CD45.2^+$ Cxcl12-cKO cells failed to compete and only constituted approximately 10% of the BM LSK population and less than 1% of the total BM cells (Figure 2E). Taken together, our data indicate that loss of Cxcl12 in BM led to increased size of the HSPC pool; however, the increase was attributed to the progenitor compartment while the long-term HSCs were actually decreased.

Stroma-secreted Cxcl12 regulates BM HSPC pool homeostasis in vitro and in vivo

Based on the mesenchymal expression pattern of Cxcl12 in BM,[5-8] we speculated that stroma-secreted Cxcl12 might govern the HSPC homeostasis. To test this, we seeded equal numbers of BM $Lin^-Sca\text{-}1^+$ cells from the CAG-EGFP mice onto the 4-OHT–treated Cxcl12-WT or Cxcl12-cKO stromal layers. 4-OHT treatment efficiently reduced the Cxcl12 mRNA and protein expression to less than 1% in the Cxcl12-cKO stroma compared with those in the wild-type stroma (supplemental Figure 1F-G). Two weeks after seeding, the $EGFP^+$ cobblestone area formation cells beneath the stromal layer were observed in the Cxcl12-WT stromal layer but were hardly seen in those seeded on the Cxcl12-cKO stroma (Figure 3A); statistical analysis revealed a 4-fold reduction of cobblestone area formation cells when samples were cultured on the Cxcl12-cKO stroma. The loss of supportive environment was also evident in LTC-IC assay where wild-type BM cells were seeded onto Cxcl12-WT or Cxcl12-cKO stroma. In this setting, there was a 3-fold decrease of the LTC-IC readout in BM samples cultured on the Cxcl12-cKO stroma compared with those cultured on the Cxcl12-WT stroma (Figure 3B).

To further investigate the significance of mesenchymal secretion of Cxcl12 in vivo, wild-type (CD45.1) BM cells were transplanted into $Cxcl12^{F/+}$;Tg or $Cxcl12^{F/-}$;Tg recipients (both CD45.2). Eight weeks after transplantation, tamoxifen was administered to ablate recipient Cxcl12 as described. Eight weeks after tamoxifen treatment, as demonstrated in Figure 3C, the percentage of donor $CD45.1^+$ LSK cells in BM and PB was still higher in Cxcl12-cKO recipients compared with those in Cxcl12-WT mice, indicating an expansion of the HSPC pool when wild-type HSPCs were repopulated in the Cxcl12-deficient environment. These results demonstrate that the maintenance of HSPC homeostasis is influenced by the stromal/mesenchymal expression of Cxcl12.

Hyperproliferation and reduced quiescent state of HSPCs upon loss of Cxcl12

In the previous section, we showed that the size of the HSPC pool was increased in Cxcl12-cKO mice. This raised the possibility of a dys-regulated HSPC proliferation. To address this question, we first performed a 3-day or 14-day BrdU-labeling assay to evaluate the HSPC proliferation. We discovered that the LSK progenitor cells were in a hyperproliferation state in Cxcl12-cKO mice (Figure 4A). The finding was also in agreement with the Ki-67 staining (supplemental Figure 3A). Meanwhile, the $Ki67^+$ percentage of PB LSK cells did not significantly change upon loss of Cxcl12 (supplemental Figure 3B). The cell-cycle distribution was further assayed by Pyronin Y/Hoechst 33342 dual staining. In Cxcl12-WT mice, 19.49% ± 3.08% of LSK cells are in the G_0 state ($Hoechst^{low}$/Pyronin Y^{low} region); however, the percentage of G_0 LSK cells was reduced to 8.26% ± 2.85% in Cxcl12-cKO mice (Figure 4B). In accordance with the in vivo finding, culture of wild-type BM cells

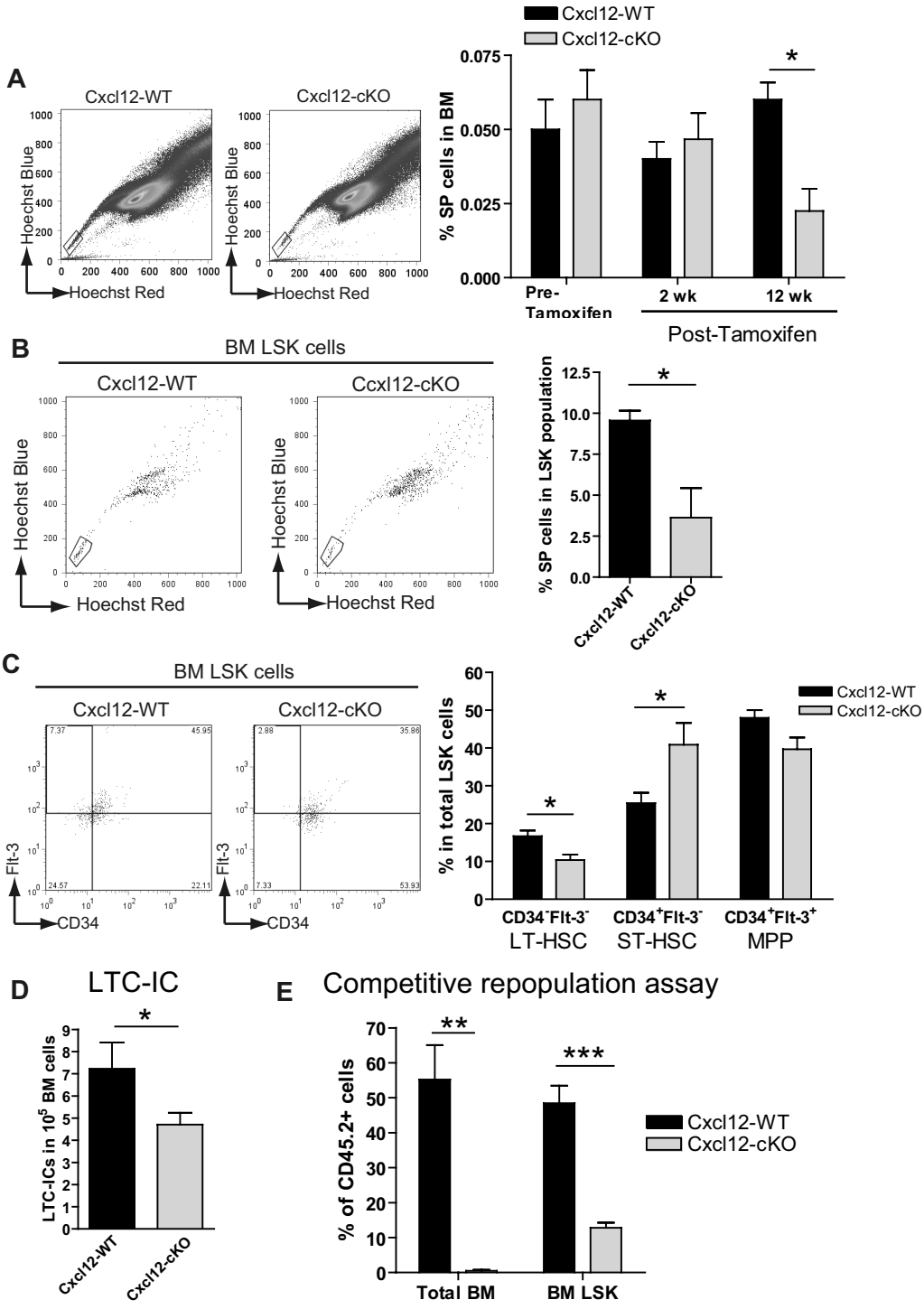

Figure 2. Increased short-term and decreased long-term HSCs upon loss of Cxcl12. (A) Representative figures of side population (SP) analysis in Cxcl12-WT and Cxcl12-cKO mice 12 weeks (wks) after tamoxifen treatment. Bar graph on the right panel shows the percentage of SP cells in BM before and after tamoxifen treatment (mean ± SEM; $*P < .05$; n = 4 each time point). (B) Representative flow cytometric results of BM SP^+LSK cells of both genotype mice 12 wks after tamoxifen treatment. Right panel shows the percentage of SP cells in LSK population in each genotype (mean ± SEM; $*P < .05$; n = 6 each). (C) Representative figures of flow cytometric analysis of Flt-3 and CD34 expression in LSK cells in Cxcl12-WT and Cxcl12-cKO mice 12 wks after tamoxifen treatment. Right panel is the percentage of $Flt\text{-}3^-CD34^-$, $Flt\text{-}3^-CD34^+$, and $Flt\text{-}3^+CD34^+$ cells in the LSK population from either genotype (mean ± SEM; $*P < .05$; n = 8 each). (D) Decreased long-term culture-initiating cell (LTC-IC) readout in BM samples (mean ± SEM; $*P < .05$; n = 7 each). (E) Competitive repopulation assay in which BM donor cells from Cxcl12-WT or Cxcl12-cKO mice (both CD45.2) were mixed 1:1 with CD45.1 competitor BM cells and transplanted into CD45.1 recipient mice. Twelve wks after transplantation, contribution of CD45.2 cells in recipient total BM or BM LSK population were analyzed (mean ± SEM; $**P < .005$, $***P < .001$; n = 4).

on the Cxcl12-cKO stroma also resulted in a decreased G_0 state of Lin^- cells compared with those seeded on the Cxcl12-WT stroma (Figure 4C). The results revealed that stroma-secreted Cxcl12 down-regulated HSPC quiescence. Loss of quiescence might be a reason why Cxcl12 deficiency led to the progenitor pool expansion while the HSCs or LTC-ICs were reduced.

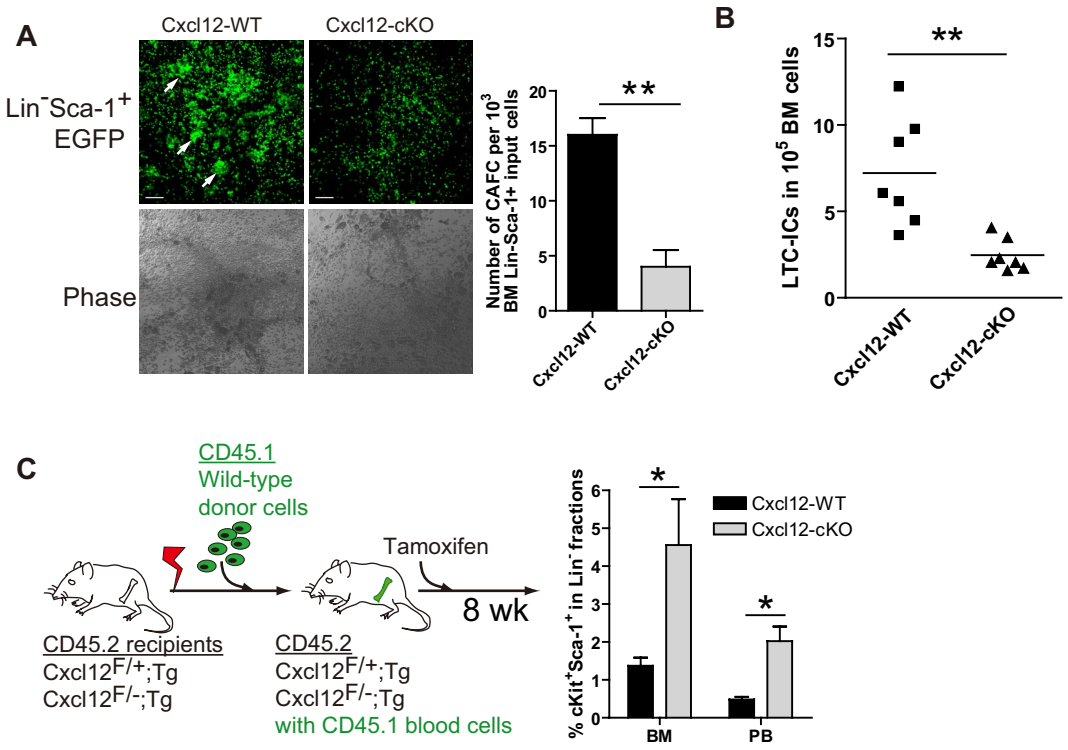

Figure 3. Cxcl12 acts as an environmental factor regulating the HSPC homeostasis. (A) Representative figures of cobblestone area formation cells (CAFCs) (arrow) derived from Cxcl12-proficient EGFP$^+$Lin$^-$Sca-1$^+$ BM cells cultured on either Cxcl12-WT or Cxcl12-cKO stromal layer. Scale bar = 100 μm. Right panel is the statistics of CAFCs readout per 2×10^3 input cells per well (mean ± SEM; $^{**}P < .005$; n = 3). (B) LTC-IC assay in which equal numbers of Cxcl12-proficient BM test cells were seeded on either Cxcl12-WT or Cxcl12-cKO stromal cell layers. The horizontal bars indicate the mean percentage ($^{**}P < .005$; n = 7). (C) Left panel is the schematic drawing of experimental strategy. The bar graph on the right panel shows the percentage of CD45.1$^+$cKit$^+$Sca-1$^+$ cells in Lin$^-$ fraction in recipients' BM and PB (mean ± SEM; $^*P < .05$; n = 4).

We also examined the expression level of other stroma-expressed factors, angiopoietin-1,[20] osteopontin,[21,22] jagged1,[23] N-cadherin,[24] and SCF,[25] which have been reported as homeostatic regulators of HSCs. Among them, the expression levels of angiopoietin-1 and SCF mRNA of Cxcl12-cKO stroma were reduced by nearly 60% and 50%, respectively, compared with the Cxcl12-WT counterpart (Figure 4D). The ELISA data further demonstrated a decrease of SCF present in the stromal culture supernatant (Figure 4E). This suggested that stroma-secreted Cxcl12 might regulate the HSPC homeostasis through either a direct or indirect mechanism.

Loss of Cxcl12 confers survival advantage and faster hematologic recovery in a myelosuppression model

To investigate the implication of Cxcl12 deficiency in a hematologic stress condition, we adapted a 5-fluorouracil (5-FU) myelosuppression model. Two weeks after tamoxifen treatment, a single dose of 5-FU (200 mg/kg body weight) was given to the Cxcl12-WT and Cxcl12-cKO mice. Unexpectedly, leukopenia was less severe in the Cxcl12-cKO mice as revealed by elevated total white blood cell (WBC), neutrophils, and lymphocytes counts (Figure 5A). In addition, recovery of BM cellularity was more efficient in the Cxcl12-cKO mice (Figure 5B). In the progenitor compartment, post–5-FU Cxcl12-cKO mice also maintained a significantly higher proportion of the BM LSK cells than Cxcl12-WT mice did (Figure 5C).

To further amplify the 5-FU resistance phenotype, a single lethal dose of 5-FU (500 mg/kg body weight) was administered to Cxcl12-WT and Cxcl12-cKO mice. Within 15 days, all 10 tested Cxcl12-WT mice were dead, while 50% Cxcl12-cKO mice survived (Figure 5D). The result revealed that Cxcl12-deficient mice gained survival advantage and showed quicker hematologic regeneration more than wild-type mice in a single dose of 5-FU challenge. The findings were accompanied by an increased number of hematopoietic progenitor cells and mature cells.

Loss of Cxcl12 leads to suppressed hematopoiesis along the bone-lining surface and ectopic BM regeneration in the perisinusoidal space upon myelosuppression

To explore the hematologic regeneration pattern in Cxcl12-cKO BM, we examined the BM histology of post–5-FU bone samples. 5-FU treatment led to a severe reduction of BM cells in both genotypes within 4 days (Figure 6Aii,vi). Later, regeneration can be observed on the endosteal surface in wild-type BM (Figure 6Aiii-iv), in agreement with the previous report that post–5-FU BM regeneration was initiated at the endosteal zone.[26] In contrast, BM regeneration along the endosteal surface was less obvious in Cxcl12-deficient mice; rather, it clearly occurred in the central space as a spheroidal cluster form, especially in the diaphysis region (Figure 6Avii-viii). We performed immunofluorescence to identify the CD150$^+$CD41$^-$CD48$^-$ long-term HSCs[27] in these clusters 7 days after the 5-FU treatment. We found that in clusters larger than 100 μm in diameter, single or multiple CD150$^+$CD41$^-$CD48$^-$ cells could be detected, and they were closely associated with CD150$^-$CD41$^+$CD48$^+$ progenitors (Figure 6B). The result revealed that an active hematopoietic regeneration did occur in these ectopic hematopoietic loci in Cxcl12-cKO mice. We next examined the distribution of the Tie2$^+$ hematopoietic cells in post–5-FU BM sections as these cells have been demonstrated as the long-term HSCs, and their association to the bone surface can

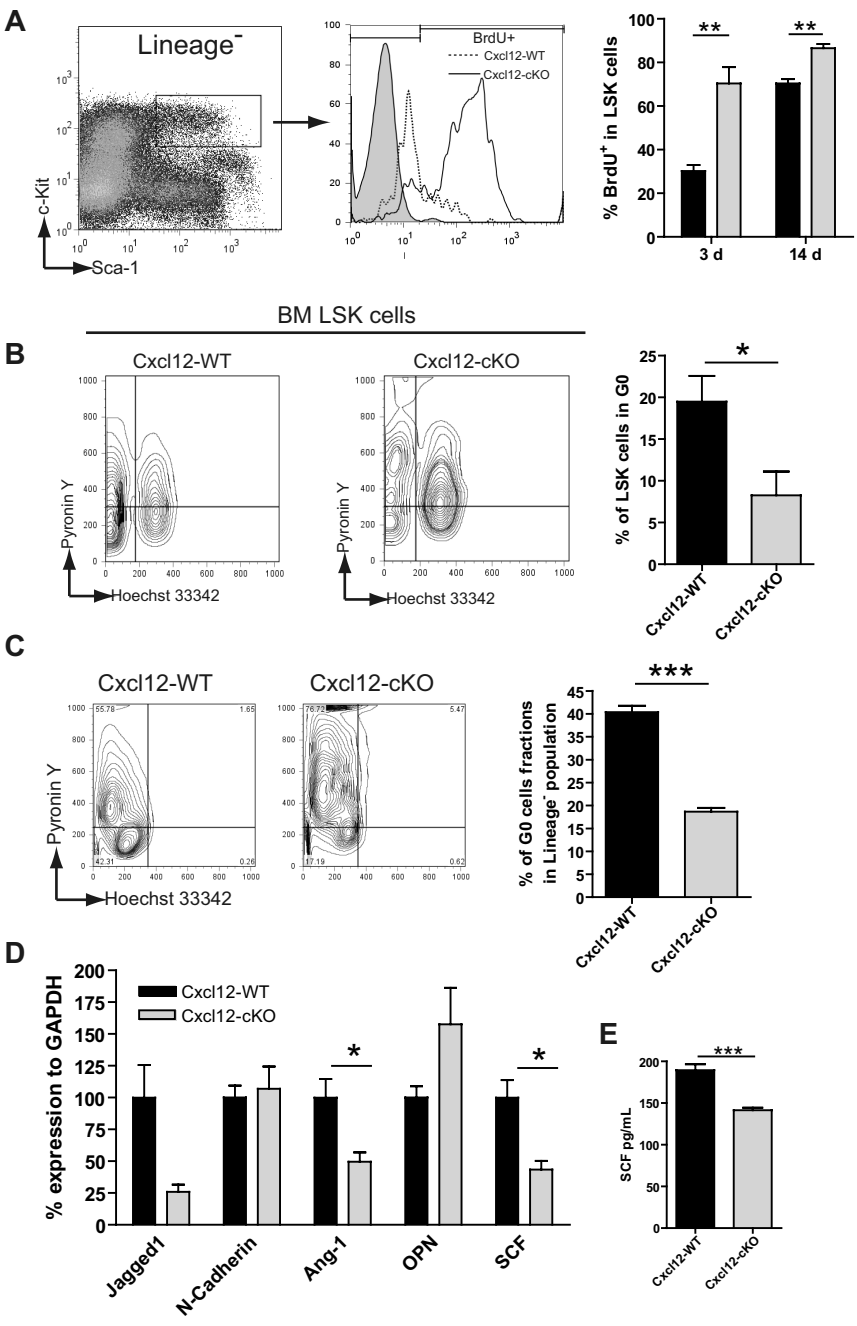

Figure 4. Loss of Cxcl12 leads to increased G_0-to-G_1 cell-cycle entry and cell proliferation of HSPC. (A) LSK cell proliferation was tested by BrdU incorporation for 3 and 14 days and assayed by flow cytometry; statistical data are presented in the right bar graph (mean ± SEM; $^{**}P < .005$; n = 6 for 3 days and n = 5 for 14 days). (B) BM LSK cells were dual-stained with Hoechst 33342 and Pyronin Y to reveal the cell-cycle status. The percentage of LSK cells in G_0 phase (Pyronin Y^{low}, 2N DNA) is demonstrated on the right bar graph (mean ± SEM; $^{*}P < .05$; n = 8 each). (C) Hoechst 33342 and Pyronin Y dual staining of 14-day culture of wild-type BM cells seeded on either Cxcl12-WT or Cxcl12-cKO stromal layer. Percentage of lineage$^-$ gated cells in G_0 phase was analyzed and is shown in the right panel (mean ± SEM; $^{***}P < .001$; n = 3). (D) Quantitative RT-PCR assay for mRNA expression level of homeostatic regulator genes in Cxcl12-WT or Cxcl12-cKO stroma (mean ± SEM; $^{*}P < .05$; n = 4). (E) ELISA test for SCF in stromal culture supernatant (mean ± SEM; $^{***}P < .001$; n = 6).

be clearly seen after the 5-FU treatment.[20] The histologic examination revealed that in Cxcl12-WT BM, $CD45.2^+Tie2^+$ cells were in close contact with the endosteal surface and were usually embedded in the newly regenerated $CD45.2^+$ cell clusters (Figure 6C). In contrast, these $Tie2^+$ HSCs were dissociated from the endosteal surface in Cxcl12-cKO BM. Statistical results demonstrated that nearly 50% of them were more than 50 μm from the bone surface (Figure 6C right panel).

The ectopic hematopoietic regeneration pattern after myelosuppression and the dissociation of $Tie\text{-}2^+$ HSCs from bone surface led us to speculate that prior to myelosuppression, the HSPC distribution in the homeostatic state could have been changed upon loss of Cxcl12. To explore this hypothesis, we examined the $CD150^+CD41^-CD48^-$ cell distribution in the homeostatic BM samples. In Cxcl12-WT BM, $CD150^+CD41^-CD48^-$ cells could be readily found in the perisinusoidal space and, to a lesser amount, along the osteocalcin-positive osteoblast-lining bone surface at the trabecular bone region (Figure 6D). Some of those bone-adhering $CD150^+CD41^-CD48^-$ long-term stem cells or $CD150^+CD41^+CD48^+$ intermediates were associated with $CD150^-CD41^+CD48^+$ progenitors (Figure 6Di-ii, white bracket). In Cxcl12-cKO BM, either $CD150^+CD41^-CD48^-$ cells or progenitor clusters were not present along the bone-surface (Figure 6Diii-iv and inset). Loss of bone adherence of the progenitor clusters was also evident when the sections were examined by cKit/Sca-1 double staining (Figure 6E). The results indicated that loss of Cxcl12 led to the dislodgment of HSPCs from the bone-lining surface and this change contributed, in part, to the ectopic BM hematopoiesis after the 5-FU myelosuppression challenge.

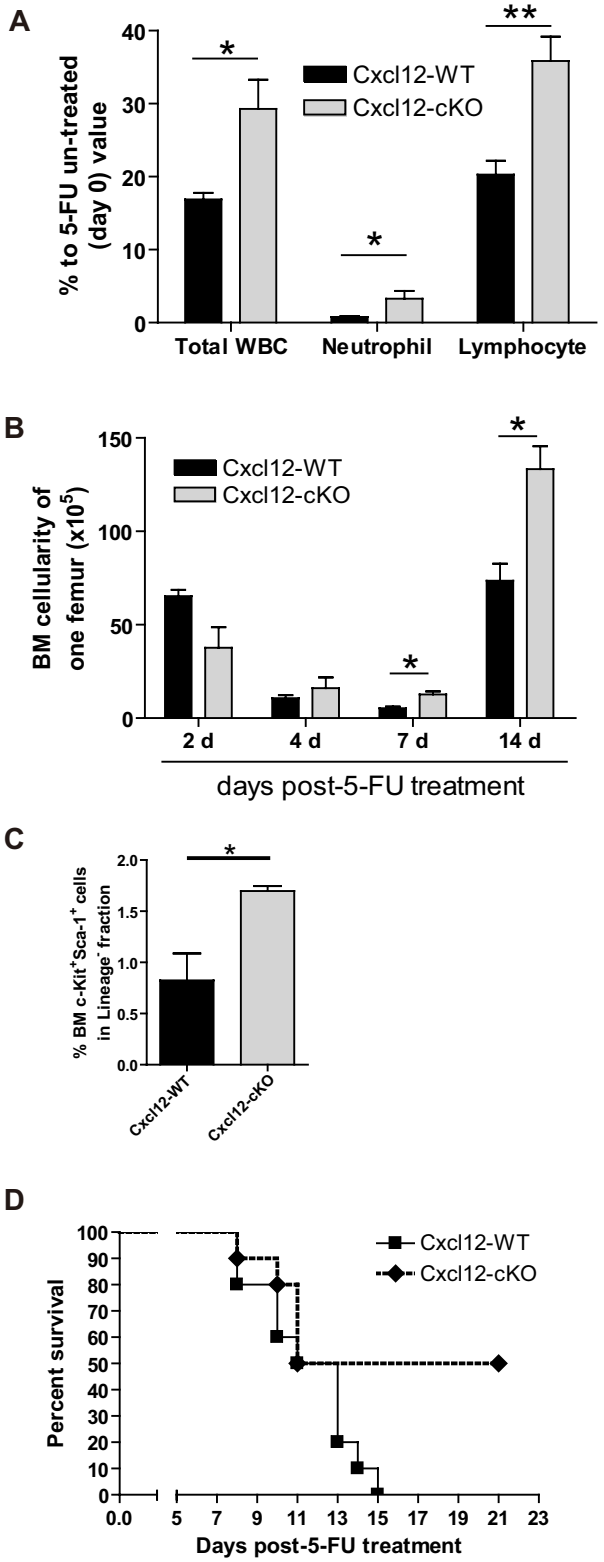

Figure 5. Loss of Cxcl12 results in faster hematologic re-establishment under 5-FU challenge in mice deficient in Cxcl12. (A) The peripheral blood profile 7 days after a single 5-FU treatment (200 mg/kg body weight) revealed that leukopenia was less severe in Cxcl12-cKO mice. Peripheral blood was collected at day 0 and day 7 after 5-FU treatment. WBC, neutrophil, and lymphocyte counts for individual mice were compared with their day-0 value (mean ± SEM; $*P < .05$, $**P < .01$; n = 8). (B) BM regeneration was demonstrated by BM cellularity recovery after 5-FU treatment. Bar graph shows the BM nucleated cells from one femur in each specific time point (mean ± SEM; $*P < .05$; each time point n = 3). (C) BM LSK cell population analysis in Cxcl12-WT and Cxcl12-cKO mice 7 days after 5-FU challenge (mean ± SEM; $*P < .05$; n = 4 each). (D) Kaplan-Meier survival curve (log rank test $P = .0484$; n = 10 each) for mice treated by a single lethal dose of 5-FU (500 mg/kg body weight).

Discussion

HSPC homeostasis is a critical issue in the hematopoietic system. In the adult BM, the diverse expression pattern of Cxcl12 suggests that it may influence the organization of stem cell niche, but this has not been tested before in a gene-deficient background. In this report, we found that: (1) loss of Cxcl12 in the adult immediately led to the expansion of hematopoietic progenitors in BM and PB; (2) stroma-secreted Cxcl12 contributed to the regulation of HSPC homeostasis; and (3) persistent loss of Cxcl12 led to reduction of long-term repopulating HSCs and loss of quiescence. Histologic examination of BM sections in homeostatic and post–5-FU state revealed that hematopoiesis was disrupted on the bone-lining surface, suggesting a defective osteoblastic microenvironment in Cxcl12-deficient mice.

Our study showed that loss of Cxcl12 in the adult immediately led to the expansion of hematopoietic progenitors in BM, PB, and in the spleen. Our study also revealed that circulating progenitors were not hyperproliferative (supplemental Figure 3B) despite being in a hyperactive cell-cycle state in BM. Therefore, the increased PB progenitors in Cxcl12-cKO mice could result from the retention defect of progenitors in BM, which led to excessive egress into the circulation. Likewise, the increased proportion of neutrophils in peripheral WBC could be due partly to the retention defect in BM, as Cxcl12 has been reported as a major retention signal for neutrophils in BM.[28]

Our data revealed that Cxcl12-deficient stromal cells were unable to support the population and quiescence of wild-type LTC-ICs. The result echoed previous studies where exogenous addition of Cxcl12 promoted the quiescence of cultured HSPCs[13] and the secondary replating capacity of cultured murine BM cells.[29] In addition, our data showed that SCF expression was decreased in Cxcl12-deficient stromal cells. Loss of the SCF receptor, Kit, leads to the increased proliferation of HSPCs and a reduction of long-term repopulating HSCs,[25] similar to the phenotype of Cxcl12 deficiency. This finding also suggests that Cxcl12 might govern the stem cell function indirectly through regulating stromal or osteoblast activity. Although this hypothesis requires further study focusing on a osteoblast tissue-specific deletion model, several indirect findings have pointed toward this possibility. In our immunofluorescence studies, we found that osteocalcin signal intensity was generally low in Cxcl12-cKO BM compared with that in the wild-type counterpart (supplemental Figure 2). Furthermore, Cxcl12 deficiency led to a loss of B-cell precursor in BM (Figure 1E); the phenomenon also occurred when osteoblasts were ablated in a Col2.3delta-TK mice model.[30,31] Cxcr4 is expressed in circulating osteoblast precursors and some osteogenic cell lines,[32,33] and Cxcl12 reduction in BM was accompanied with suppression of osteoblast activity.[9] It is therefore possible that the Cxcl12 might regulate osteoblast activity through an autocrine or paracrine mechanism in vivo.

Our data also revealed that Cxcl12-deficient mice possessed increased hematopoietic progenitors and a better survival rate upon lethal dose of 5-FU challenge. We reasoned that the survival advantage was due to the quicker rebuild of BM cellularity and peripheral WBCs, which was partly contributed to by the increased proliferation of the progenitor population originating from quiescent stem cells. We also speculate that BM recovery from the single dose of 5-FU challenge might depend on the recovery of total HSPC population, since the speeded BM regeneration was also evident 3 months after Cxcl12 ablation (data not shown), at the

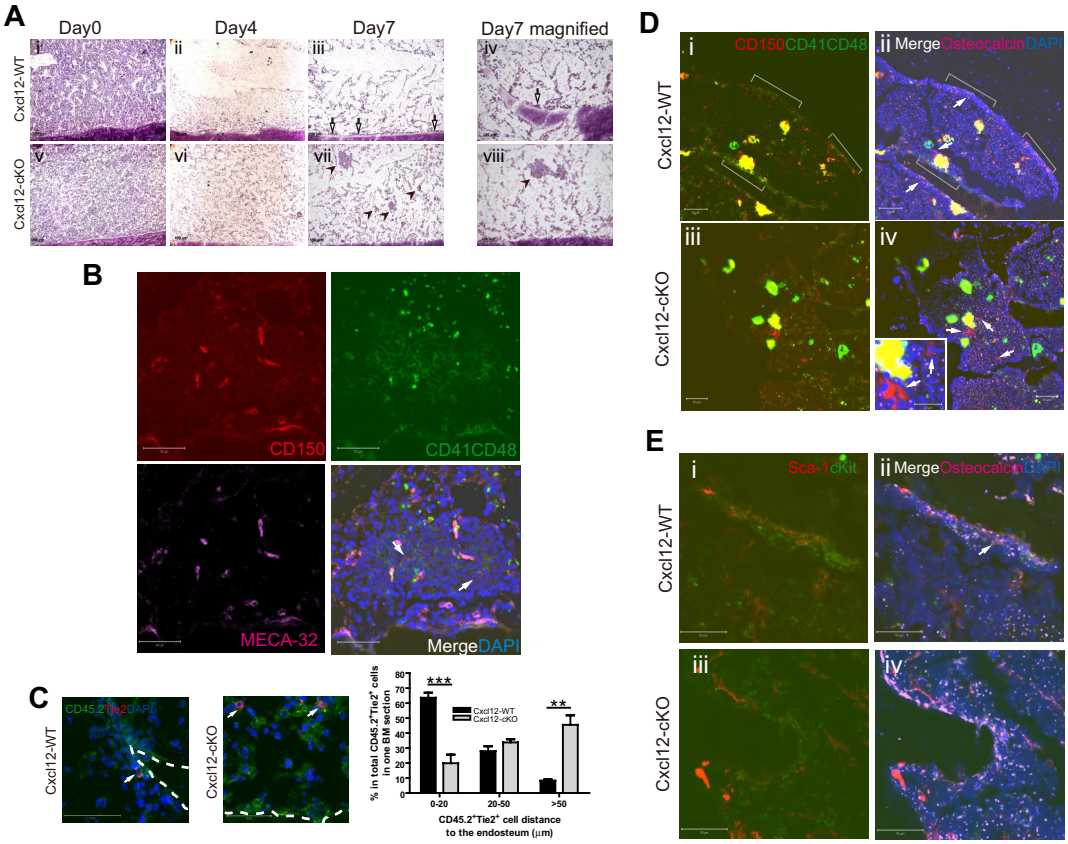

Figure 6. Loss of HSPC attachment to endosteal zone and ectopoic BM hematopoietic loci upon myelosuppression in Cxcl12-deficient mice. (A) Hematoxylin-eosin staining of BM section of Cxcl12-WT (i-iv) and Cxcl12-cKO (v-viii) mice at various time point after 5-FU treatment. Hematopoietic cell clusters from endosteal surface (arrow) or from perisinusoidal space (arrowhead) are indicated. The magnified pictures (iv,viii) show the ectopic site of BM regeneration in Cxcl12-cKO mice. Scale bar = 100 μm. (B) Representative figure of the regenerated perisinusoidal cell cluster in Cxcl12-cKO BM stained with CD150/CD41/CD48 and endothelial marker MECA-32. $CD150^+CD41^-CD48^-$ cells (red, arrow) were identified, and they were associated with $CD150^+CD41^+CD8^+$ (yellow) and $CD150^-CD41^+CD48^+$ (green) progenitors. Scale bar = 50 μm. (C) Four days after 5-FU treatment, $CD45.2^+Tie2^+$ HSCs (arrow) can be seen along the endosteal surface in Cxcl12-WT BM, but they were scattered in perisinusoidal region in Cxcl12-cKO BM. Dotted line indicates the endosteal surface. Scale bar = 50 μm. For statistics, $CD45.2^+Tie2^+$ cells per BM section were measured for their distance (in microns) to the nearest endosteal surface. The percentage in respect of such distance was analyzed and is presented in the right penal (mean ± SEM; $^{**}P < .005$, $^{***}P < .001$; n = 4). (D) Representative figures of CD150/CD41/CD48/osteocalcin immunofluorescence on Cxcl12-WT (i-ii) and Cxcl12-cKO (iii-iv) BM at homeostatic state. The $CD150^+CD41^-CD48^-$ cells are indicated by arrow. The inset is the higher magnification for $CD150^+CD41^-CD48^-$ cells in Cxcl12-cKO samples. In Cxcl12-WT BM, some of them were associated with $CD150^-CD41^+CD48^+$ and $CD150^+CD41^+CD48^+$ progenitor cluster along the bone lining surface (white bracket), but in Cxcl12-cKO BM, these hematopoietic clusters were not detected. Scale bar = 50 μm; inset scale bar = 20 μm. (E) Immunostaining for cKit/Sca-1 combined with osteocalcin on Cxcl12-WT (i-ii) and Cxcl12-cKO (iii-iv) BM at homeostatic state. $cKit^+Sca\text{-}1^+$ cells (arrow) can be seen along the bone-lining surface, usually within a $cKit^+$ cell cluster, but it was absent at bone-lining surface of Cxcl12-cKO samples. Scale bar = 50 μm.

time the long-term HSCs population had already decreased. Nevertheless, it would be interesting in the future to use a more rigorous challenge model such as total BM ablation by irradiation after BM transplantation to investigate the dependence of Cxcl12 in maintaining the survival of long-term HSCs.

It was reported previously that the BM sinusoidal system was compromised after 5-FU treatment or irradiation; the transplanted donor stem cells were involved in the reconstruction of a normal sinusoid system.[34,35] Accordingly, in post–5-FU Cxcl12-deficient BM, the preferential localization of HSPCs in the perisinusoidal space might contribute to the quicker rebuild of a vasculature-related environment for hematopoiesis. Compared with the wild-type mice, Cxcr4-deficient mice had a low survival rate after serial doses of 5-FU challenge,[8,13] while the same challenge did not result in a significant survival difference in Cxcl12-deficient mice (data not shown). An earlier study reported that the post–5-FU hematopoietic and thrombocytic regeneration was significantly disrupted when mice were treated by anti-Cxcr4 antibodies; histologic examination demonstrated an absence of hematopoiesis on either the bone-lining surface or in the perisinusoidal space.[36] To explain this, we postulated that the regeneration either on the endosteal surface or in the perisinusoidal space were both disrupted in Cxcr4-deficient mice, which accounts for the low survival rate upon myelosuppression. It also hints that in adult BM HSCs, Cxcr4 could mediate other signaling systems which are probably independent of Cxcl12, and these Cxcr4-mediated signaling systems are critical for organizing the perisinusoidal niche in the regenerating BM.

In addition to the homeostatic imbalance phenotype, we also found that HSPCs were not attached to the bone-lining surface in Cxcl12-cKO mice; the finding was accompanied by a change of hematopoietic site from the bone-lining surface to perisinusoidal space upon 5-FU myelosuppression. Based on these findings, we proposed that loss of Cxcl12 in physiologic state significantly affects the organization of the osteoblastic niche, which leads to the dislodgement of HSPCs from the osteoblast-lining bone surface (Figure 7). According to these findings, we postulate that other than the direct loss of Cxcl12-Cxcr4 signaling, the detachment of HSPCs from the osteoblastic niche also accounts for their dysregulated homeostasis. Osteoblasts are a major source of several quiescent factors; therefore, detachment from the bone-lining surface could make the HSPCs deprived of these quiescent signals emanating from osteoblasts.

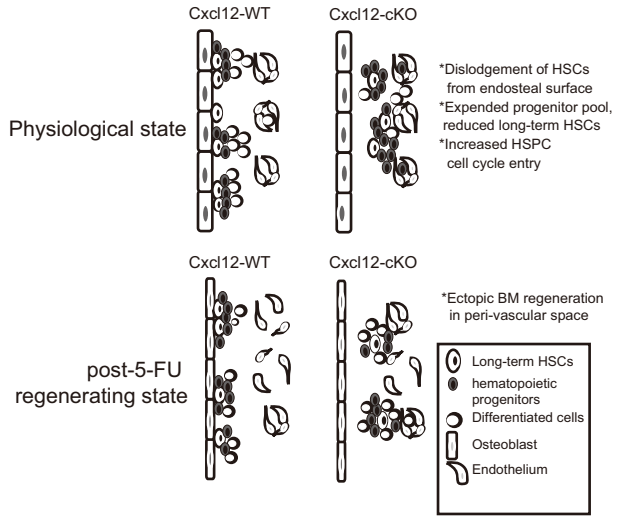

Figure 7. Summary of Cxcl12-deficiency phenotype in adult BM. Loss of Cxcl12 in adult BM resulted in expansion of hematopoietic progenitor pools accompanied with gradual loss of long-term HSCs and excessive cell-cycle entry. In Cxcl12-deficient BM, bone-adhering HSPCs were absent, suggesting a disruption of osteoblastic niche organization. The absence of hematopoiesis from osteoblastic niche was also evident as revealed by the finding that post–5-FU BM regeneration mostly occurred in perisinusoidal space rather than bone-lining surface in Cxcl12-cKO mice.

What kind of stem cell niches are responsible for supporting hematopoiesis in Cxcl12-deficient BM? In our current study we could not find a direct answer due to the anatomic complexity in the central marrow space. However, the ectopic loci of BM hematopoietic regeneration indirectly revealed that in Cxcl12-deficient mice, hematopoiesis was highly dependent on the niches located in the perisinusoidal region. It has been proposed that the bone-lining surface is a preferred place for primitive HSCs,[37] while the perivascular region provides a permissive environment for progenitors' expansion.[38] Accordingly, the expanded progenitor pool observed in Cxcl12-deficient mice could partly reflect the niche's characteristics in the perivascular space. Recently, Sugiyama et al[8] identified a certain type of Cxcl12-abundant reticular cell (CAR cell) that might constitute a novel stem cell niche in BM. Due to their proximity to the osteoblast-lining bone surface, the CAR cells could also participate in organizing the osteoblastic niche. The loss of progenitor clusters along the bone surface upon loss of Cxcl12 could be attributed to the loss of their attachment to the CAR cells as well. It would be important in the future to identify the surface markers of such reticular cells to further investigate their role in HSPC niche transition upon loss of Cxcl12.

In conclusion, we have developed a novel genetic model that unravels the critical role of Cxcl12 in postnatal hematopoiesis. The stroma-secreted Cxcl12 keeps the HSCs in a quiescent state and retains them in the osteoblastic niche. Our model also provides a new research tool for studying stem cell behavior in different BM niche locations.

Acknowledgments

We thank the Taiwan Mouse Clinic, funded by the National Research Program for Genomic Medicine at the National Science Council of Taiwan (NSC 98-3112-B-001-020), for performing peripheral blood cell profiles. We thank Mrs. Ya-Min Lin in the flow cytometry core of the Institute of Molecular Biology for cell sorting. We thank Dr. Che-Kun James Shen and the Research Center of Medical Excellence of National Taiwan University for providing the research facility. We also thank Dr. Nan-Shih Liao, Dr. Li-Ru You, and Dr. Harry Wilson for editing the paper and discussion.

This work was supported by the National Science Council of Taiwan (NSC 95-2745-B-001-001-MY3 and NSC 98-2314-B-002-042-MY3) and MOEA of Taiwan (98-EC-17-A-01-S1-131).

This paper is presented in the memory of Dr Hung Li of the Institute of Molecular Biology, Academia Sinica, who was the former principal investigator of the Cxcl12 project.

Authorship

Contribution: Y.S.T, Y.L.K, W. C. Chen, and W. C. Cheng performed experiments and analyzed data; and Y.S.T. and D.M.L. designed the research and wrote the paper.

Conflict-of-interest disclosure: The authors declare no competing financial interests.

Correspondence: Dar-Ming Lai, Division of Neurosurgery, Department of Surgery, National Taiwan University Hospital, Taipei 100, Taiwan; e-mail: dmdlai@ntu.edu.tw; or Yi-Shiuan Tzeng, Institute of Molecular Biology, Academia Sinica, Taipei 115, Taiwan; e-mail: yishiuan@imb.sinica.edu.tw.

References

1. Zhang J, Li L. Stem cell niche: microenvironment and beyond. *J Biol Chem.* 2008;283(15):9499-9503.
2. Kiel MJ, Morrison SJ. Uncertainty in the niches that maintain haematopoietic stem cells. *Nat Rev Immunol.* 2008;8(4):290-301.
3. Orkin SH, Zon LI. Hematopoiesis: an evolving paradigm for stem cell biology. *Cell.* 2008;132(4):631-644.
4. Broxmeyer HE. Chemokines in hematopoiesis. *Curr Opin Hematol.* 2008;15(1):49-58.
5. Ponomaryov T, Peled A, Petit I, et al. Induction of the chemokine stromal-derived factor-1 following DNA damage improves human stem cell function. *J Clin Invest.* 2000;106(11):1331-1339.
6. Semerad CL, Christopher MJ, Liu F, et al. G-CSF potently inhibits osteoblast activity and Cxcl12 mRNA expression in the bone marrow. *Blood.* 2005;106(9):3020-3027.
7. Sipkins DA, Wei X, Wu JW, et al. In vivo imaging of specialized bone marrow endothelial microdomains for tumour engraftment. *Nature.* 2005;435(7044):969-973.
8. Sugiyama T, Kohara H, Noda M, Nagasawa T. Maintenance of the hematopoietic stem cell pool by Cxcl12-Cxcr4 chemokine signaling in bone marrow stromal cell niches. *Immunity.* 2006;25(6):977-988.
9. Katayama Y, Battista M, Kao WM, et al. Signals from the sympathetic nervous system regulate hematopoietic stem cell egress from bone marrow. *Cell.* 2006;124(2):407-421.
10. Nakayama T, Mutsuga N, Tosato G. FGF2 post-transcriptionally down-regulates expression of SDF1 in bone marrow stromal cells through FGFR1 IIIc. *Blood.* 2007;109(4):1363-1372.
11. Nagasawa T, Hirota S, Tachibana K, et al. Defects of B-cell lymphopoiesis and bone-marrow myelopoiesis in mice lacking the CXC chemokine PBSF/SDF-1. *Nature.* 1996;382(6592):635-638.
12. Zou YR, Kottmann AH, Kuroda M, Taniuchi I, Littman DR. Function of the chemokine receptor Cxcr4 in haematopoiesis and in cerebellar development. *Nature.* 1998;393(6685):595-599.
13. Nie Y, Han YC, Zou YR. Cxcr4 is required for the quiescence of primitive hematopoietic cells. *J Exp Med.* 2008;205(4):777-783.
14. Goodell MA, Brose K, Paradis G, Conner AS, Mulligan RC. Isolation and functional properties of murine hematopoietic stem cells that are replicating in vivo. *J Exp Med.* 1996;183(4):1797-1806.
15. Ladd AC, Pyatt R, Gothot A, et al. Orderly process of sequential cytokine stimulation is required for activation and maximal proliferation of primitive human bone marrow CD34+ hematopoietic progenitor cells residing in G0. *Blood.* 1997;90(2):658-668.
16. Hayashi S, McMahon AP. Efficient recombination in diverse tissues by a tamoxifen-inducible form of Cre: a tool for temporally regulated gene activation/inactivation in the mouse. *Dev Biol.* 2002;244(2):305-318.
17. Ara T, Tokoyoda K, Sugiyama T, Egawa T,

Kawabata K, Nagasawa T. Long-term hematopoietic stem cells require stromal cell-derived factor-1 for colonizing bone marrow during ontogeny. *Immunity.* 2003;19(2):257-267.

18. Yang L, Bryder D, Adolfsson J, et al. Identification of Lin(-)Sca1(+)kit(+)CD34(+)Flt3- short-term hematopoietic stem cells capable of rapidly reconstituting and rescuing myeloablated transplant recipients. *Blood.* 2005;105(7):2717-2723.
19. van Os R, Kamminga LM, de Haan G. Stem cell assays: something old, something new, something borrowed. *Stem Cells.* 2004;22(7):1181-1190.
20. Arai F, Hirao A, Ohmura M, et al. Tie2/angiopoietin-1 signaling regulates hematopoietic stem cell quiescence in the bone marrow niche. *Cell.* 2004; 118(2):149-161.
21. Nilsson SK, Johnston HM, Whitty GA, et al. Osteopontin, a key component of the hematopoietic stem cell niche and regulator of primitive hematopoietic progenitor cells. *Blood.* 2005;106(4): 1232-1239.
22. Stier S, Ko Y, Forkert R, et al. Osteopontin is a hematopoietic stem cell niche component that negatively regulates stem cell pool size. *J Exp Med.* 2005;201(11):1781-1791.
23. Calvi LM, Adams GB, Weibrecht KW, et al. Osteoblastic cells regulate the haematopoietic stem cell niche. *Nature.* 2003;425(6960):841-846.
24. Zhang J, Niu C, Ye L, et al. Identification of the haematopoietic stem cell niche and control of the niche size. *Nature.* 2003;425(6960):836-841.
25. Thoren LA, Liuba K, Bryder D, et al. Kit regulates maintenance of quiescent hematopoietic stem cells. *J Immunol.* 2008;180(4):2045-2053.
26. Heissig B, Hattori K, Dias S, et al. Recruitment of stem and progenitor cells from the bone marrow niche requires MMP-9 mediated release of kit-ligand. *Cell.* 2002;109(5):625-637.
27. Kiel MJ, Yilmaz OH, Iwashita T, Yilmaz OH, Terhorst C, Morrison SJ. SLAM family receptors distinguish hematopoietic stem and progenitor cells and reveal endothelial niches for stem cells. *Cell.* 2005;121(7):1109-1121.
28. Suratt BT, Petty JM, Young SK, et al. Role of the Cxcr4/SDF-1 chemokine axis in circulating neutrophil homeostasis. *Blood.* 2004;104(2):565-571.
29. Broxmeyer HE, Mejia JAH, Hangoc G, Barese C, Dinauer M, Cooper S. SDF-1/Cxcl12 enhances in vitro replating capacity of murine and human multipotential and macrophage progenitor cells. *Stem Cells Dev.* 2007;16(4):589-596.
30. Visnjic D, Kalajzic Z, Rowe DW, Katavic V, Lorenzo J, Aguila HL. Hematopoiesis is severely altered in mice with an induced osteoblast deficiency. *Blood.* 2004;103(9):3258-3264.
31. Zhu J, Garrett R, Jung Y, et al. Osteoblasts support B-lymphocyte commitment and differentiation from hematopoietic stem cells. *Blood.* 2007; 109(9):3706-3712.
32. Otsuru S, Tamai K, Yamazaki T, Yoshikawa H, Kaneda Y. Circulating bone marrow-derived osteoblast progenitor cells are recruited to the bone-forming site by the Cxcr4/stromal cell-derived factor-1 pathway. *Stem Cells.* 2008;26(1): 223-234.
33. Zhu W, Boachie-Adjei O, Rawlins BA, et al. A novel regulatory role for stromal-derived factor-1 signaling in bone morphogenic protein-2 osteogenic differentiation of mesenchymal C2C12 cells. *J Biol Chem.* 2007;282(26):18676-18685.
34. Hooper AT, Butler JM, Nolan DJ, et al. Engraftment and reconstitution of hematopoiesis is dependent on VEGFR2-mediated regeneration of sinusoidal endothelial cells. *Cell Stem Cell.* 2009; 4(3):263-274.
35. Slayton WB, Li XM, Butler J, et al. The role of the donor in the repair of the marrow vascular niche following hematopoietic stem cell transplant. *Stem Cells.* 2007;25(11):2945-2955.
36. Avecilla ST, Hattori K, Heissig B, et al. Chemokine-mediated interaction of hematopoietic progenitors with the bone marrow vascular niche is required for thrombopoiesis. *Nat Med.* 2004;10(1): 64-71.
37. Lo Celso C, Fleming HE, Wu JW, et al. Live-animal tracking of individual haematopoietic stem/progenitor cells in their niche. *Nature.* 2009;457(7225):92-96.
38. Kopp HG, Avecilla ST, Hooper AT, Rafii S. The bone marrow vascular niche: home of HSC differentiation and mobilization. *Physiology.* 2005;20(5): 349-356.